

## Supporting Information

# Nanopore modified with stimuli-responsive polymer for measuring $\beta$ -amyloid peptide and zinc ions in brains of live mice with Alzheimer's disease

Shushu Ding,<sup>a,b</sup> Yue Zhu,<sup>a</sup> Anwei Zhu,<sup>b</sup> Guoyue Shi<sup>\*,b</sup>

<sup>a</sup> School of Pharmacy, Nantong University, 19 Qixiu Road, Nantong 226001, People's Republic of China

<sup>b</sup> School of Chemistry and Molecular Engineering, Shanghai Key Laboratory for Urban Ecological Processes and Eco-Restoration, East China Normal University, 500 Dongchuan Road, Shanghai 200241, People's Republic of China

## **Table of contents**

1. Synthesis and characterization of the derivative of sialic acid (Figure S1-S3)
2. Synthesis and characterization of the derivative of quinoline (AQZ) (Figure S4-S6)
3. Synthesis and characterization of PNI-TP-SA-AQZ (Figure S7-S9)
4. Characterization of glass nanopore (Figure S10-S11)
5. Contact angle experiment (Figure S12)
6. Optimized conditions (Figure S13)
7. The reproducibility of the glass nanopore (Figure S14)
8. Interferences and competition test for the determination of A $\beta$  monomers and Zn<sup>2+</sup> (Figure S15)
9. Comparison of the performance of different methods for the determination of A $\beta$  monomers (Table S1)

## Reagents and materials

Gold(III) chloride trihydrate ( $\text{HAuCl}_4 \cdot 3\text{H}_2\text{O}$ ), cation exchange resin, potassium iodide (KI), sodium sulphate ( $\text{Na}_2\text{SO}_4$ ), sodium bicarbonate ( $\text{NaHCO}_3$ ) and 2,2'-azobis(isobutyronitrile) (AIBN) were purchased from Sinopharm Chemical Reagent Co., Ltd. Boron (tri)fluoride etherate ( $\text{BF}_3 \cdot \text{OEt}_2$ ), hydroxyethyl methacrylate (HEMA), 2-(2-aminoethoxy) ethanol, 8-aminoquinoline, 2-chloroacetyl chloride, *N,N*-diisopropylethylamine, sodium borohydride ( $\text{NaBH}_4$ ) and all metallic salts were supplied by Aladdin. Sialic acid (SA), *N*-isopropylacrylamide (NIPAAm), S-benzyl dithiobenzoate (BDTB), proteins and amino acids were purchased from Sigma-Aldrich. Acryloyl-3,5-bis(trifluoromethyl)-phenylthiourea (Ac-TP) was synthesized based on the method previously reported.<sup>1</sup>  $\beta$ -Amyloid peptides were purchased from ChinaPeptides Co., Ltd (Shanghai, China).  $\text{A}\beta$  monomer solution was prepared by mixing  $\text{A}\beta_{40}$  and  $\text{A}\beta_{42}$  in a ratio of 6:1. The oligomeric forms of  $\text{A}\beta$  were prepared by incubating  $\text{A}\beta$  monomer solution in PBS at 37 °C for 24 h.<sup>2</sup> Artificial cerebrospinal fluid (aCSF) was prepared according to the reported method.<sup>3</sup> Borosilicate glass capillary (1 mm o.d., 0.78 mm i.d.) was purchased from Sutter Instrument Co..

## Apparatus

Scanning electron microscope (Hitachi S-4800) and transmission electron microscope (JEOL JEM-2100) were employed to obtain the morphology of glass nanopore, energy-dispersive X-ray (EDX) spectrum and elemental mappings. X-ray photoelectron spectrometer (XPS) was obtained by a Kratos Axis Ultra DLD

spectrometer. Fourier transform infrared (FT-IR) spectra were supplied by NEXUS 670 spectrometer. The hydrogen nuclear magnetic resonance ( $^1\text{H}$  NMR) spectra were acquired from the Bruker AV-500 instrument. Atomic force microscope (AFM) images were provided by the Bruker Multimode 8 system.

### **Synthesis of the derivative of sialic acid (SA)**

According to reported method,<sup>4</sup> firstly, sialic acid (0.8 g) and cation exchange resin (1.6 g) were dissolved in 20 mL of methanol. The reaction mixture was stirred at ambient temperature for 24 h. Then, the filtrate was dried with anhydrous  $\text{Na}_2\text{SO}_4$  overnight. After filtration, the product 1 as white powder was obtained by reduced pressure distillation and vacuum drying.

Secondly, the product 1 and acetic anhydride (molar ratio 1:10) were dissolved in 10 mL of pyridine at 0 °C. After reaction at room temperature for 24 h, hydrochloric acid (1M) was added dropwise until the pH of the solution decreased to 2. The mixture was extracted with ethyl acetate. The organic layer was washed with saturated sodium bicarbonate until the pH of the solution increased to 7. The organic layer was dried over anhydrous  $\text{Na}_2\text{SO}_4$  overnight. After filtration, the product 2 as white powder was obtained by reduced pressure distillation and vacuum drying.

Finally, the product (2), HEMA and molecular sieve (4 A) was dissolved in 10 mL of dry dichloromethane ( $\text{CH}_2\text{Cl}_2$ ) under nitrogen atmosphere. Then,  $\text{BF}_3 \cdot \text{OEt}_2$  was added dropwise into the mixture, which was stirred for 24 h at ambient temperature (product 2 : HEMA :  $\text{BF}_3 \cdot \text{OEt}_2 = 1 : 1.5 : 4.5$ ). Then, the reaction mixture was poured

into ice water. After filtration, the mixture was extracted with  $\text{CH}_2\text{Cl}_2$ . The organic layer was washed with saturated  $\text{NaHCO}_3$  and deionized water to neutral. After being dried over anhydrous  $\text{Na}_2\text{SO}_4$  overnight, the product 3 (SA) was obtained by reduced pressure distillation.

### **Synthesis of the derivative of quinoline (AQZ)**

According to reported method,<sup>5</sup> firstly, 8-aminoquinoline (0.29 g) and pyridine (0.22 g) were dissolved in 10 ml of chloroform. Then, 2-chloroacetyl chloride (0.46 g) was added dropwise at 0 °C within 1 h. After stirred at ambient temperature for 2 h, the mixture was removed under reduced pressure to obtain a white solid (product 4), which was purified by silica gel column chromatography using dichloromethane as eluent.

Secondly, the above product 4 (0.1 g), 2-(2-aminoethoxy)ethanol (0.75 g), *N,N*-diisopropylethylamine (0.59 g) and potassium iodide (0.01 g) were added to 30 ml of acetonitrile. After stirred and refluxed for 10 h under nitrogen atmosphere, the mixture was cooled to room temperature and the solvent was removed under reduced pressure. Then, silica gel column chromatography using chloroform/methanol (20:1, v/v) as eluent was used to obtain product 5.

Finally, the product 5 (0.6 g) and triethylamine (0.3 g) were dissolved in 20 mL of dichloromethane. Then, acryloyl chloride (0.3 g) was added dropwise at 0 °C. After being stirred at ambient temperature for 12 h, the mixture was washed with distilled water. The organic layer was dried overnight in anhydrous  $\text{Na}_2\text{SO}_4$ . After evaporation of solvent, the crude product was purified on a silica gel column, with elution of

CHCl<sub>3</sub>/CH<sub>3</sub>OH (20:1, v/v), to give yellow oil (product 6, AQZ).

### **Synthesis of copolymer (PNI-TP-SA-AQZ)**

Copolymer was synthesized by reversible addition-fragmentation chain transfer (RAFT) polymerization. Firstly, NIPAAm, AC-TP, SA, AQZ, BDTB and AIBN (molar ratio 180:20:20:20:2:1) were dissolved in 1 mL of 1,4-dioxane. After being degassed three times, the mixture was stirred at 70°C for 24 h. Then, the reaction was halted by the addition of chloroform and the copolymer was precipitated by the addition of ethyl ether. The product was redissolved with chloroform and then precipitated with ethyl ether. This precipitation procedure was repeated three times. The purified product with light pink color were dried under vacuum overnight.

Secondly, the above product (200 mg) was dissolved in 10 mL of methanol / water (1:1). Then, sodium methoxide (1M) was added to adjust the value of pH to 9. After the reaction mixture was stirred at ambient temperature for 24 h, cation exchange resin (2.5 g) was added to adjust the value of pH to 7. Finally, the mixture was dried over anhydrous Na<sub>2</sub>SO<sub>4</sub> overnight. After evaporation of solvent, the product (PNI-TP-SA-AQZ) was obtained. The number-average molecular weight  $M_n$  was estimated by gel permeation chromatography (GPC) as 14323 ( $M_w/M_n = 1.15$ ).

### **Preparation of copolymer modified glass nanopores**

Firstly, the glass capillaries were washed with freshly prepared piranha solution (98% H<sub>2</sub>SO<sub>4</sub>: 30% H<sub>2</sub>O<sub>2</sub> = 3:1) and then rinsed with a large amount of deionized water and

dried at 80° C. The glass capillaries were pulled by a CO<sub>2</sub>-laser-based pipette puller (P-2000, Sutter Instrument) to produce conical glass nanopores with the following parameters: Heat=320, Fil=4, Vel=40, Del=180, Pull =225.

Then, Au thin film was decorated on the inner surface of glass nanopore by one-step photochemical approach.<sup>6</sup> Subsequently, copolymer was immobilized onto the above surface via Au-S bond. Briefly, PNI-SA-TP-AQZ (55 mg) and NaBH<sub>4</sub> solution (550 μL, 100 mM) were dissolved in methanol (10 mL). The mixture was reacted overnight at 4 °C to obtain copolymer with sulfhydryl group. Then, the above solution was backfilled into the glass nanopore and kept overnight, followed by rinsing with methanol and distilled water.

### **Ionic current measurement**

The recording range of current voltage (*I-V*) curve is -1V~ +1V, and the voltage step amplitude is 50 mV. During the test, the Ag/AgCl electrode in the nanochannel was used as the working electrode, while the reference/counter electrode (Ag/AgCl) was placed outside the glass capillary. The electrolyte solution used for measuring the *I-V* curve is 10 mM KCl solution (the buffer is Tris-HCl, pH=7.4). Each test was repeated five times to obtain the average current at different voltages.

### **In vivo microdialysis**

All experiments involving animals were performed following the approval of the Animal Ethics Committee of Nantong University and performed in accordance with the

ARRIVE guidelines. Male C57BL/6J mice and APP/PS1 double transgenic mice at 8 months of age were housed on a 12:12 h light-dark schedule with food and water ad libitum. The animals were anaesthetized with sodium pentobarbital (50 mg kg<sup>-1</sup>, i.p.) and positioned onto a stereotaxic frame. The microdialysis probe was implanted in the hippocampus (bregma -2.3 mm, 2.5 mm lateral to midline, and 1.8 mm below dura). Next, the aCSF solution was infused at the flow rate of 2.0 µL/min. After equilibration for 90 min, the microdialysates were collected. To determine Aβ monomers and Zn<sup>2+</sup> in microdialysates, the glass nanopore was firstly immersed into the microdialysates and then *I-V* curve was recorded in 10 mM KCl solution.

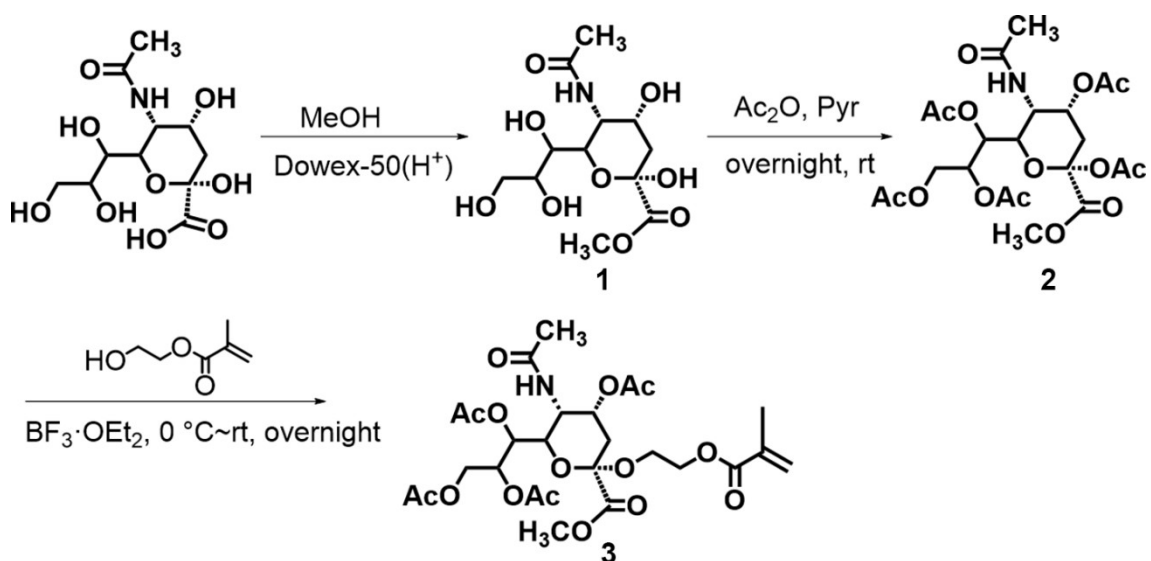


**Figure S1.** Synthetic route to the derivative of SA (product 3).

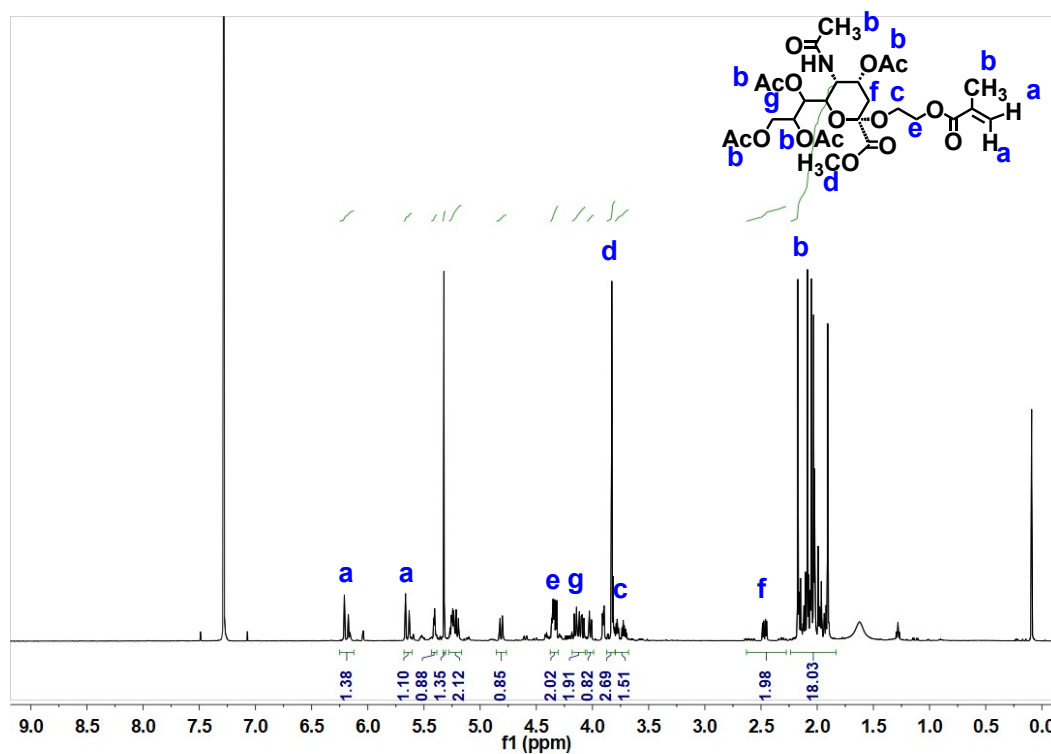
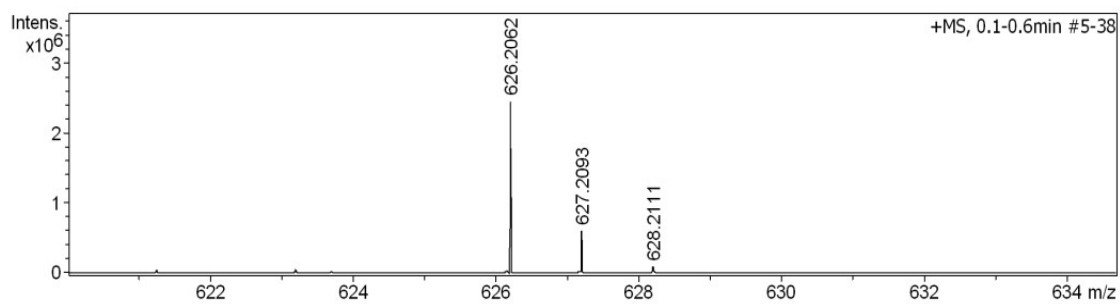


**Figure S2.**  $^1\text{H}$  NMR spectrum of the derivative of SA (product 3).

$^1\text{H}$  NMR (500 MHz,  $\text{CDCl}_3$ ):  $\delta$  6.21 – 6.17 (m, 1H), 5.67 – 5.63 (m, 1H), 5.40 (dt,  $J = 8.8, 4.4$  Hz, 1H), 5.32 (s, 1H), 5.26 – 5.21 (m, 2H), 4.80 (dd,  $J = 12.4, 2.5$  Hz, 1H), 4.35 – 4.32 (m, 2H), 4.16 – 4.09 (m, 2H), 4.03 (dd,  $J = 10.6, 2.3$  Hz, 1H), 3.82 (s, 3H), 3.80 – 3.68 (m, 2H), 2.47 (dd,  $J = 13.0, 4.9$  Hz, 2H), 2.19 – 1.87 (m, 18H).



#	m/z	Res.	S/N	I	I %	FWHM
1	626.2062	51460	122839.8	2444491	100.0	0.0122
2	627.2093	49157	30205.5	601629	24.6	0.0128
3	628.2111	34066	4085.5	81410	3.3	0.0184

Meas. m/z	#	Ion Formula	m/z	err [ppm]	mSigma	Score	rdb	e <sup>-</sup> Conf	N-Rule
626.2062	1	C <sub>26</sub> H <sub>37</sub> NNaO <sub>15</sub>	626.2055	-1.0	31.8	2	100.00	8.5	even ok

**Figure S3.** Mass spectrum of the derivative of SA (product 3).

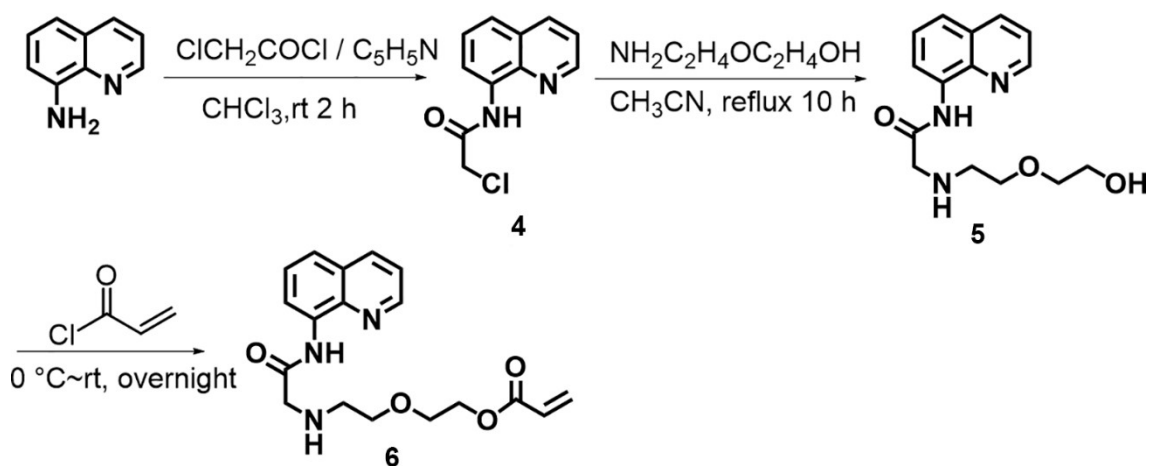


**Figure S4.** Synthetic route to the derivative of quinoline (AQZ, product 6).

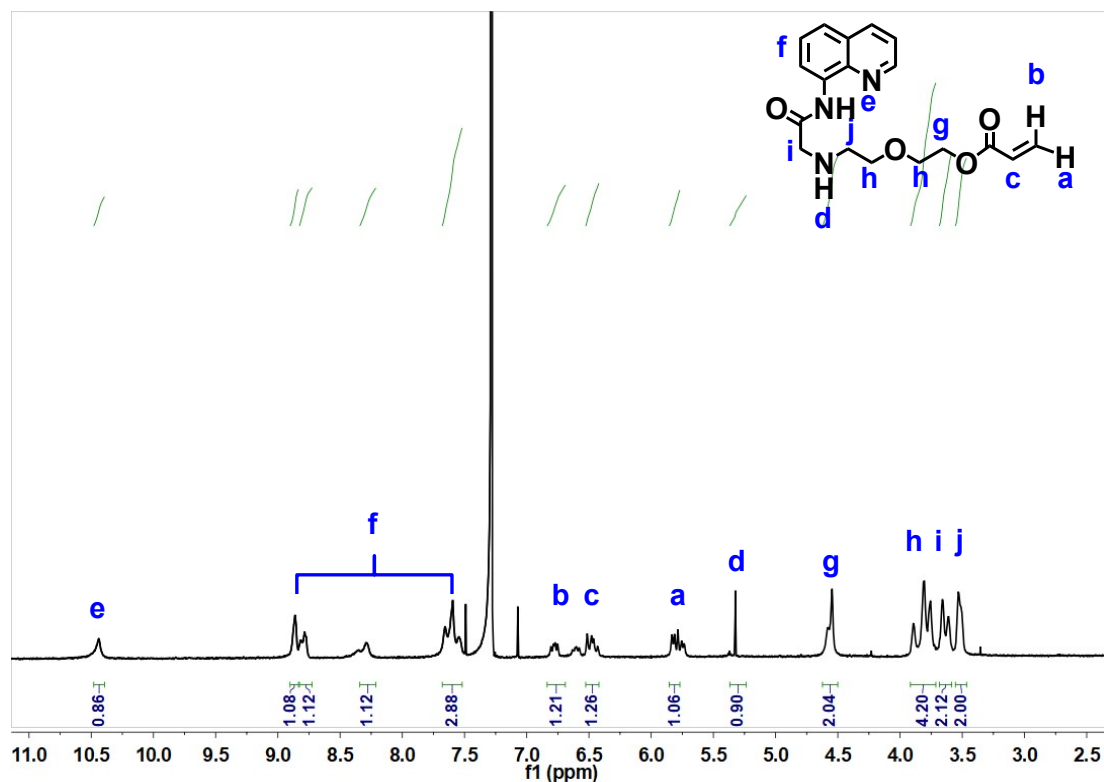
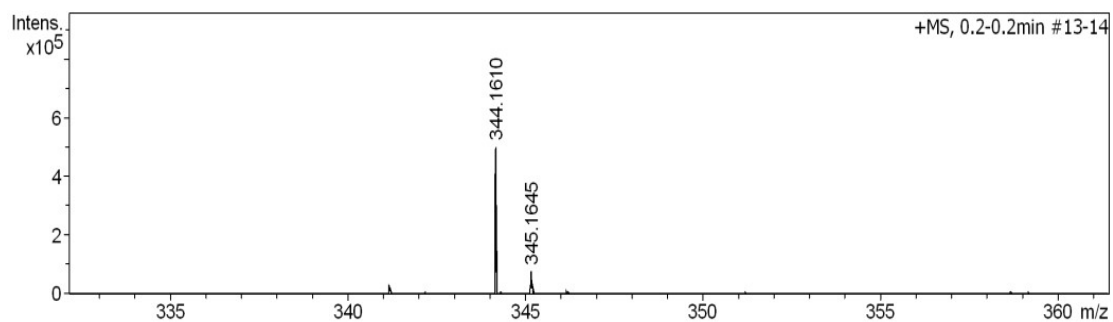


**Figure S5.** <sup>1</sup>H NMR spectrum of AQZ.

<sup>1</sup>H NMR (500 MHz, CDCl<sub>3</sub>): δ 10.44 (s, 1H), 8.82 (d,  $J = 38.7$  Hz, 2H), 8.29 (s, 1H), 7.60 (t,  $J = 28.1$  Hz, 3H), 6.73 (dd,  $J = 56.4, 46.1$  Hz, 1H), 6.47 (dd,  $J = 25.4, 16.8$  Hz, 1H), 5.87 – 5.66 (m, 1H), 5.32 (s, 1H), 4.55 (s, 2H), 3.82 (t,  $J = 34.4$  Hz, 4H), 3.64 (d,  $J = 24.4$  Hz, 2H), 3.53 (s, 2H).



#	m/z	Res.	S/N	I	I %	FWHM
1	344.1610	35252	3551.3	500998	100.0	0.0098
2	345.1645	24244	554.4	78346	15.6	0.0142
3	346.1671	15503	56.3	7974	1.6	0.0223

Meas. m/z	#	Ion Formula	m/z	err [ppm]	mSigma	Score	rdb	e <sup>-</sup> Conf	N-Rule
344.1610	1	C <sub>18</sub> H <sub>22</sub> N <sub>3</sub> O <sub>4</sub>	344.1605	-1.4	31.7	1	100.00	9.5	even ok

**Figure S6.** Mass spectrum of AQZ.

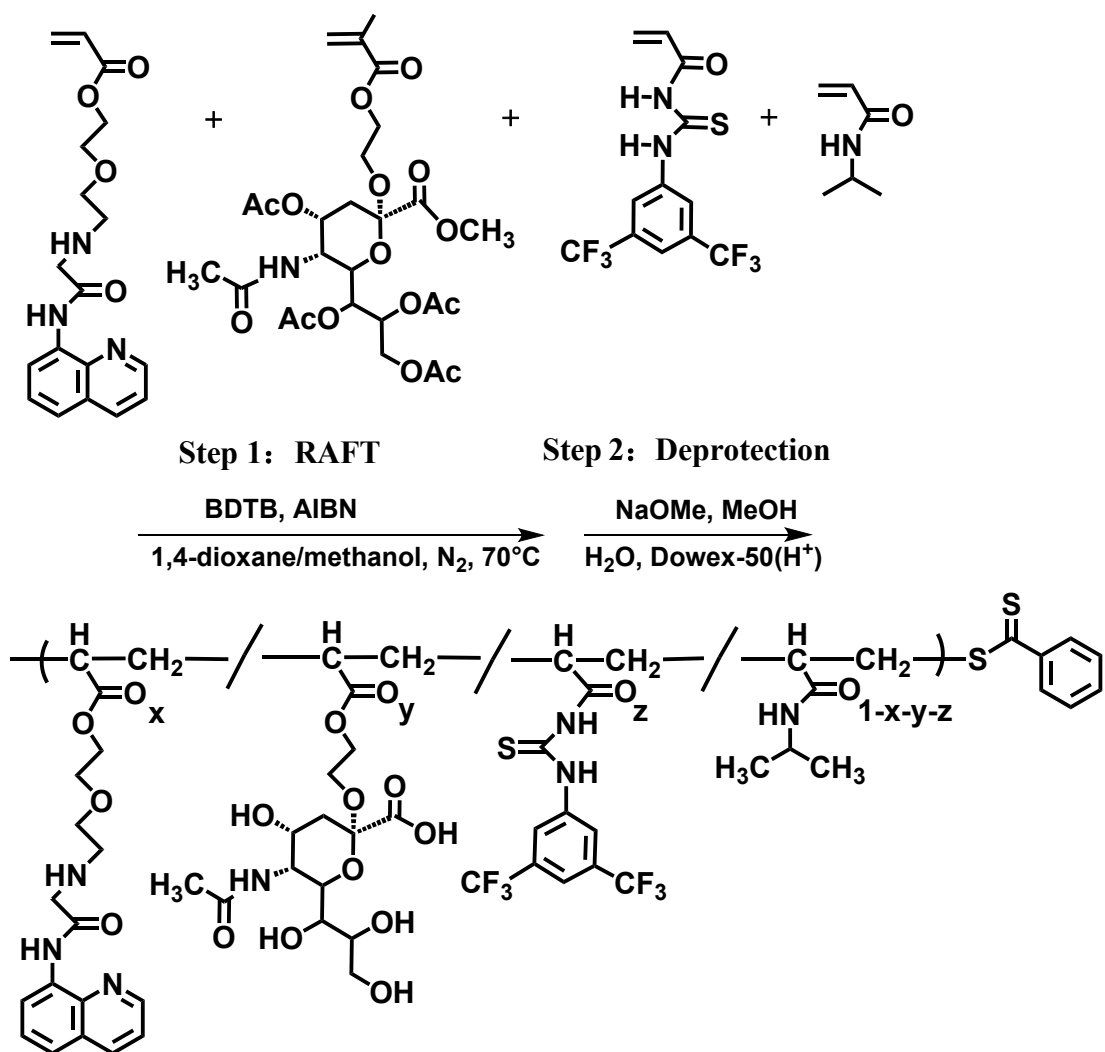
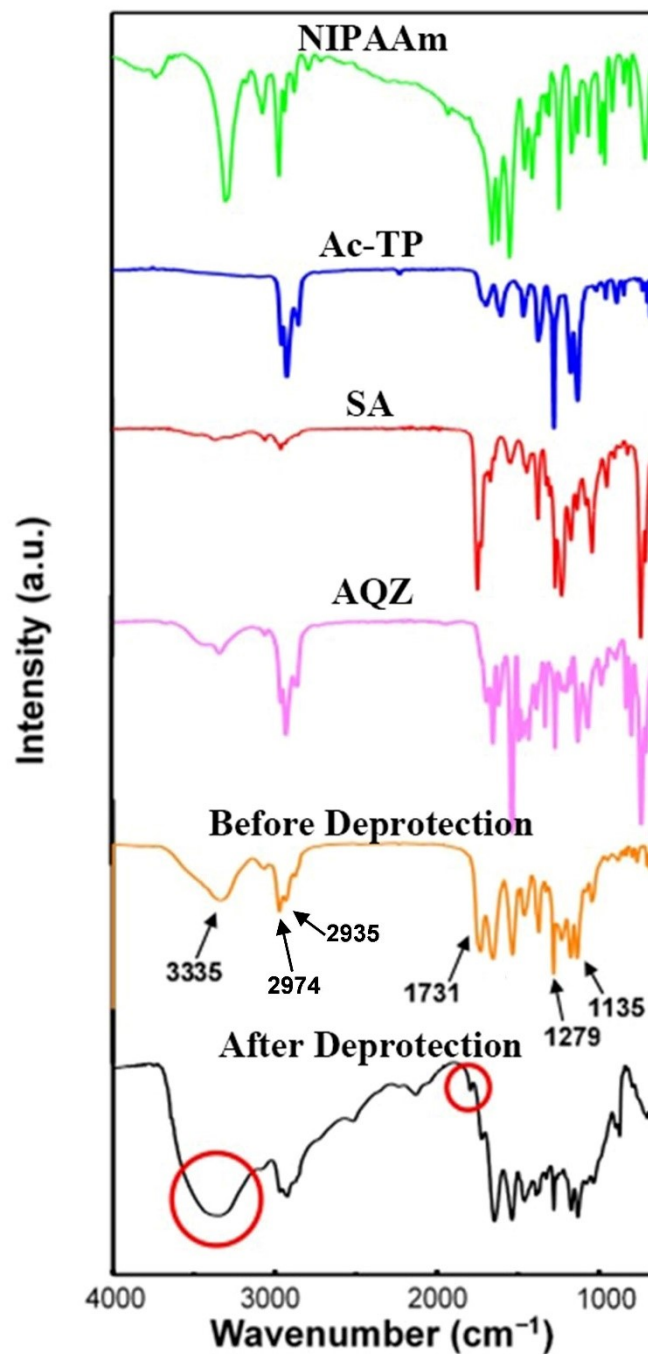
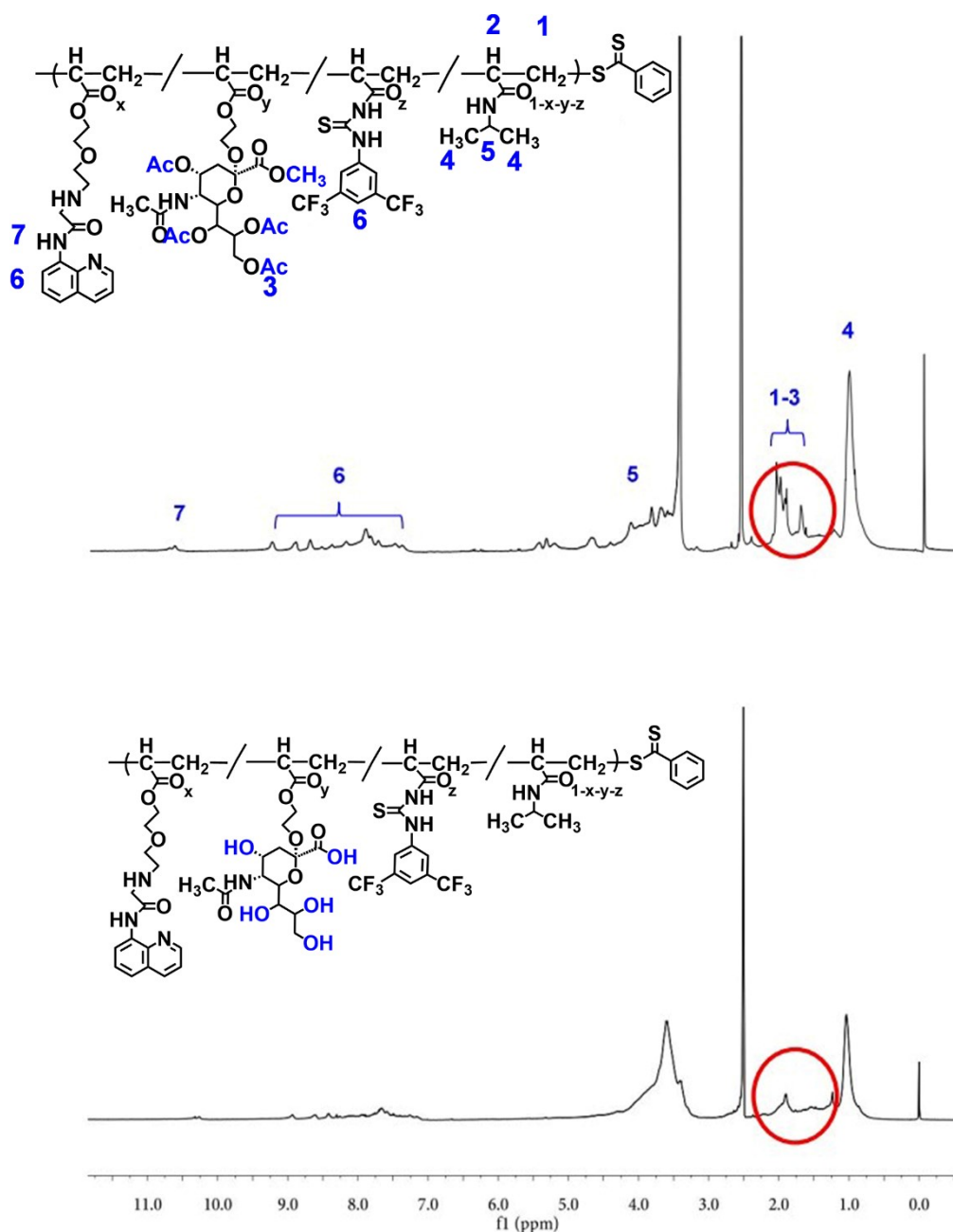


Figure S7. Synthetic route to PNI-TP-SA-AQZ



**Figure S8.** FT-IR spectra of NIPAAm (green line), Ac-TP (blue line), SA (red line), AQZ (purple line), polymer (before deprotection, orange line) and polymer (after deprotection, black line).



**Figure S9.** <sup>1</sup>H NMR spectrum of PNI-TP-SA-AQZ copolymer in CDCl<sub>3</sub>. The peak located at 10.26 ppm corresponded to the protons of amide group in AQZ unit. The signal at 7.0-8.8 ppm corresponded to the protons of phenyl group in TP unit and AQZ unit. The peak observed at 3.9 ppm and 1.1 ppm was ascribed to the protons of CH(CH<sub>3</sub>)<sub>2</sub> in NIPAAm unit. In addition, the peaks located at 2.0-1.5 ppm were attributed to the protons of acetyl group (-Ac) in SA unit and methine protons (-CH) and methylene protons (-CH<sub>2</sub>) in the backbone. After deprotection, the peak at 2.0-1.5 ppm decreased, indicating the remove of acetyl group.

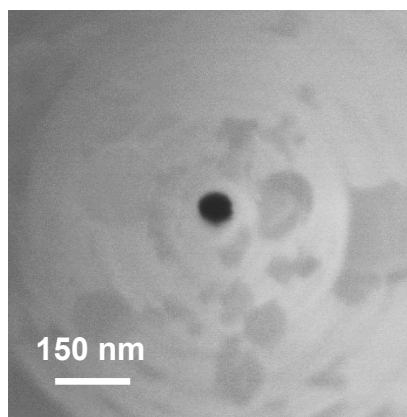


**Figure S10.** SEM image of the unmodified glass nanopore tip.

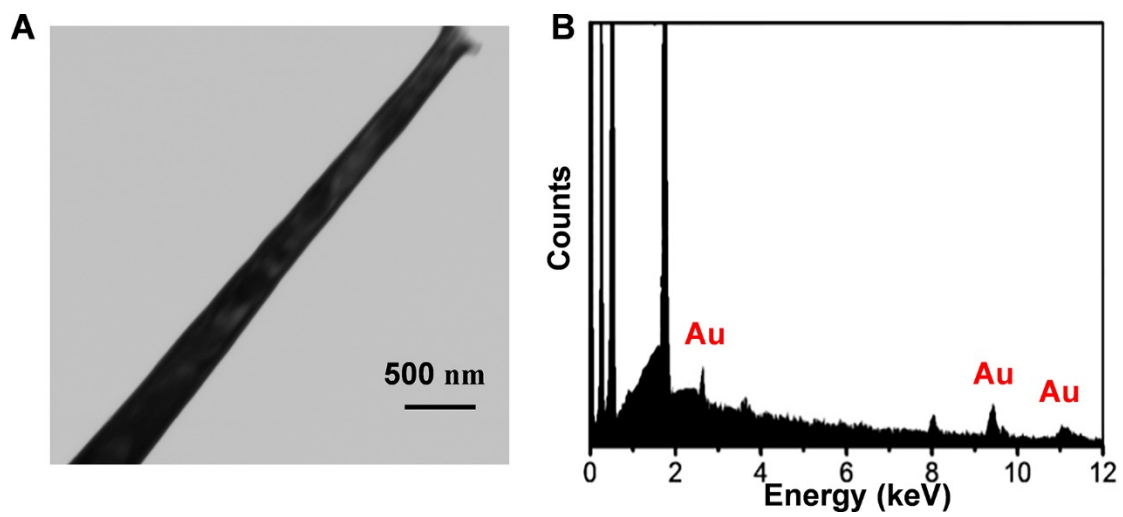


**Figure S11.** (A) Medium-magnification TEM image and (B) EDX spectra of the Au film-modified glass nanopore.

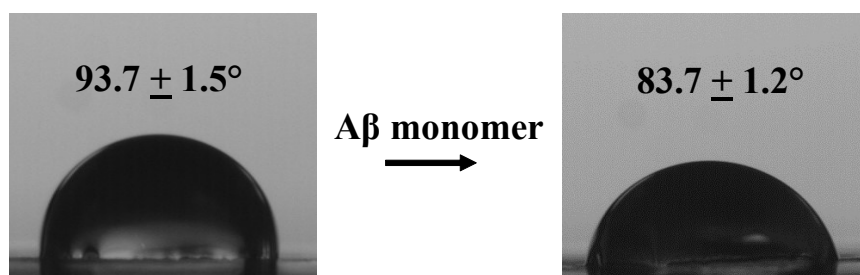


**Figure S12.** Contact angle photographs obtained at the copolymer-modified surface before (left) and after (right) the treatment of  $10^{-6}$  M A $\beta$  monomer solution.

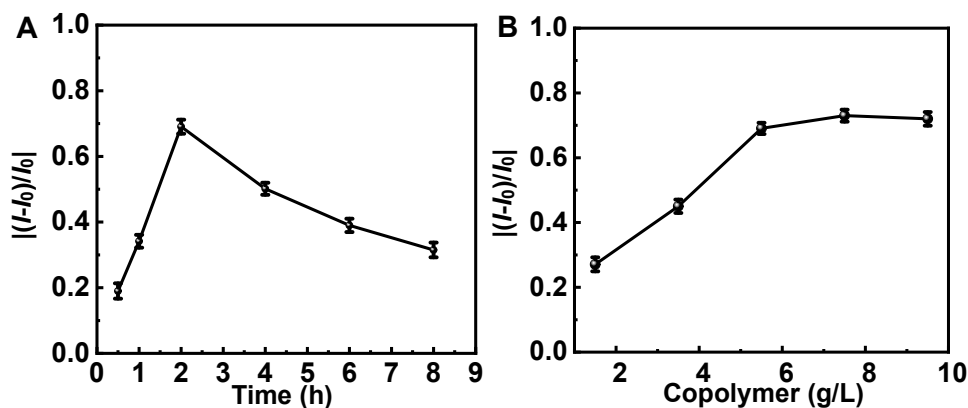


**Figure S13.** Effect of (A) the irradiation time of UV light and (B) the concentration of copolymer on the detection of  $10^{-9}$  M A $\beta$  monomers.

The Au film was decorated on the inner surface of glass nanopore by one-step photochemical approach. The thickness of Au layer is determined by irradiation time of UV light. Therefore, we explored the effect of the thickness of Au layer by changing irradiation time. As shown in Figure S13A, the ratio of ionic current change at -1.0 V ( $|(-I-I_0)/I_0|$ ) reached a maximum value when the irradiation time was 2 h, and then gradually decreased. This should be ascribed to the fast growth of Au particles in solutions, blocking off sharp tip of the nanopipette. Therefore, 2 h UV irradiation time was selected for obtaining ultrathin Au films with high quality.

As shown in Figure S13B, the ratio of ionic current change at -1.0 V ( $|(-I-I_0)/I_0|$ ) increased to maximum values when the concentration of copolymer was 5.5 g/L. Then, the ratio values kept almost unchanged, which indicated the adsorption of copolymer was saturated. Hence, the optimal concentration of copolymer was 5.5 g/L.

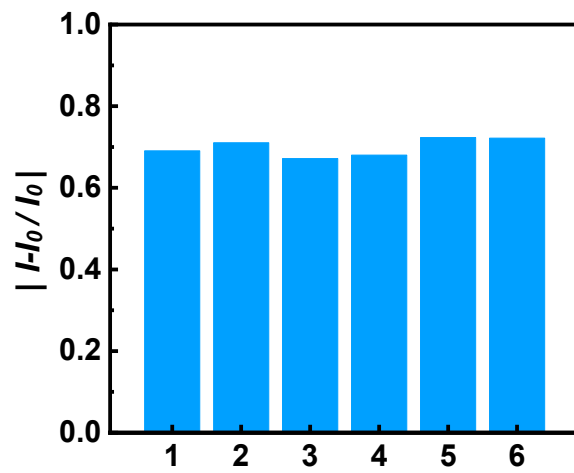


**Figure S14.** The ionic current responses of six different copolymer-modified glass nanopores toward  $10^{-9}$  M A $\beta$  monomers.

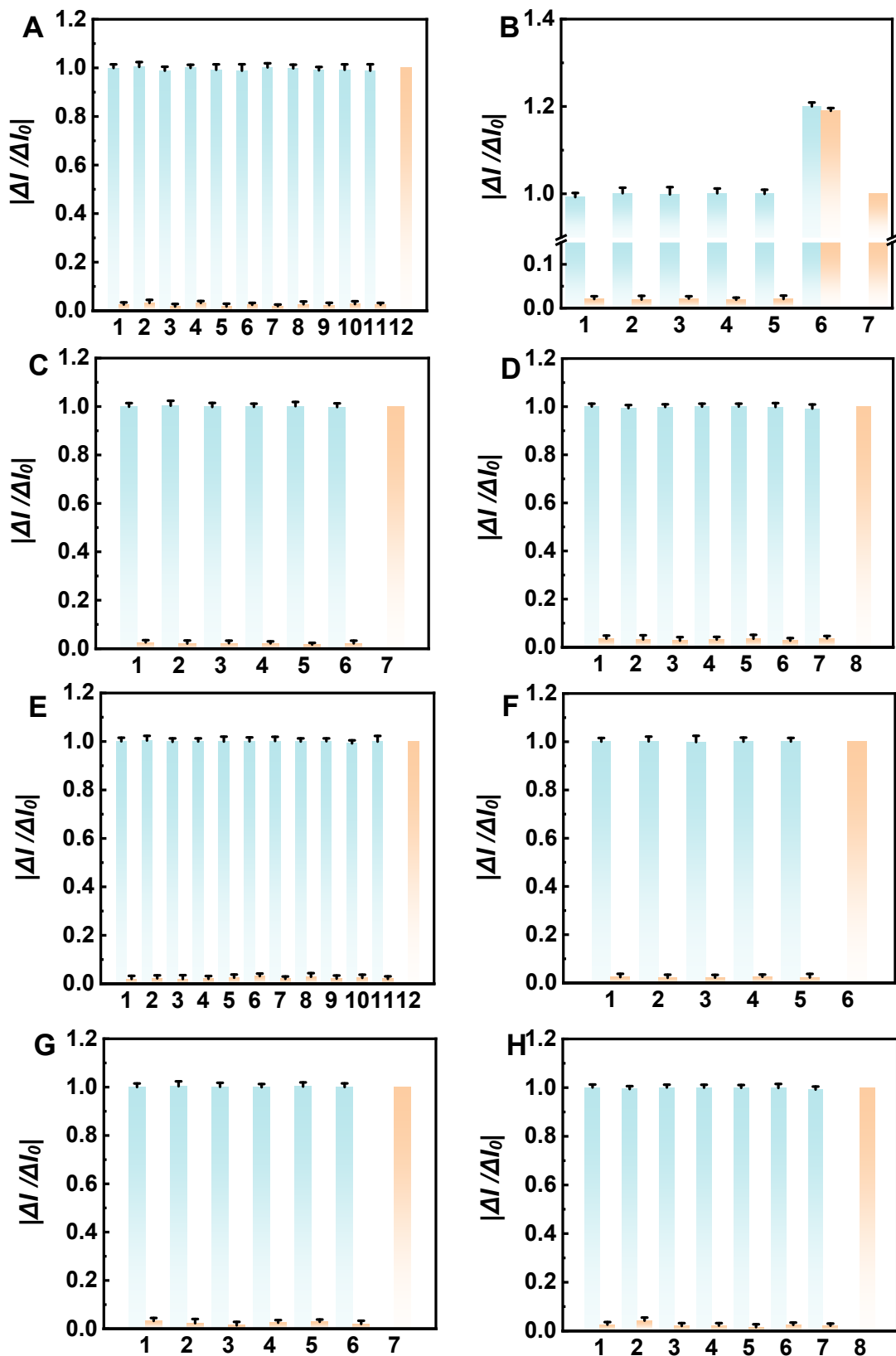


**Figure S15.** Selectivity and competition experiments of amino acids against (A) Aβ monomers (1–12: Glu, Gly, Phe, Ser, Val, Cys, His, Iso, Arg, Lys, Thr, Aβ monomers, 10 μM for all the tested amino acids, 0.1 nM for Aβ monomers) and (E) Zn<sup>2+</sup> (1–12: Glu, Gly, Phe, Ser, Val, Cys, His, Iso, Arg, Lys, Thr, Zn<sup>2+</sup>, 10 μM for all the tested

amino acids, 1 nM for  $Zn^{2+}$ ); proteins against (B) A $\beta$  monomers (1–7: Tau, Actin,  $\alpha$ -syn, Pre, VDAC1, A $\beta$  oligomers, A $\beta$  monomers, 0.1 nM for A $\beta$  monomers and oligomers, 0.2 mg mL<sup>-1</sup> for other proteins) and (F)  $Zn^{2+}$  (1–6: Tau, Actin,  $\alpha$ -syn, Pre, VDAC1,  $Zn^{2+}$ , 0.2 mg mL<sup>-1</sup> for other proteins, 1 nM for  $Zn^{2+}$ ); metal ions against (C) A $\beta$  monomers (1–7: K<sup>+</sup>, Ca<sup>2+</sup>, Na<sup>+</sup>, Mg<sup>2+</sup>, Fe<sup>3+</sup>, Cu<sup>2+</sup>, A $\beta$  monomers, 1 mM for K<sup>+</sup>, Ca<sup>2+</sup>, Na<sup>+</sup>, Mg<sup>2+</sup>; 10  $\mu$ M for Fe<sup>3+</sup> and Cu<sup>2+</sup>, 0.1 nM for A $\beta$  monomers) and (G)  $Zn^{2+}$  (1–7: K<sup>+</sup>, Ca<sup>2+</sup>, Na<sup>+</sup>, Mg<sup>2+</sup>, Fe<sup>3+</sup>, Cu<sup>2+</sup>,  $Zn^{2+}$ , 1 mM for K<sup>+</sup>, Ca<sup>2+</sup>, Na<sup>+</sup>, Mg<sup>2+</sup>; 10  $\mu$ M for Fe<sup>3+</sup> and Cu<sup>2+</sup>, 1 nM for  $Zn^{2+}$ ); Other biological molecules against (D) A $\beta$  monomers (1–8: 50  $\mu$ M AA, 20  $\mu$ M UA, 20  $\mu$ M DA, 50  $\mu$ M DOPAC, 20  $\mu$ M 5-HT, 1 mM glucose, 1 mM lactate, 0.1 nM A $\beta$  monomers) and (H)  $Zn^{2+}$  (1–8: 50  $\mu$ M AA, 20  $\mu$ M UA, 20  $\mu$ M DA, 50  $\mu$ M DOPAC, 20  $\mu$ M 5-HT, 1 mM glucose, 1 mM lactate, 1 nM  $Zn^{2+}$ ). The orange bars mean the addition of potential interferences. The blue bars mean the subsequent addition of A $\beta$  monomers or  $Zn^{2+}$ .  $\Delta I_0$  represents the current change induced by A $\beta$  monomers or  $Zn^{2+}$ ,  $\Delta I$  represents the current change induced by potential interferences or the mixture of potential interference and A $\beta$  monomers/ $Zn^{2+}$ .

**Table S1** Comparison of the performance of different methods for the determination of A $\beta$  monomers

Method	Linear range (nM)	Limit of detection (nM)	Ref.
Capillary electrophoresis	$5 \times 10^3$ - $2.6 \times 10^4$	500	7
Capillary isotachopheresis-mass spectrometry	0.06-2	0.03	8
Colorimetry (Antibody)	0.25-150	0.086	9
Fluorescence (Lanthanide-based infinite coordination polymer nanoparticles)	0.5 -100	0.17	10
Surface enhanced raman spectroscopy	0.1-0.74	0.07	11
Microfluidics (Antibody)	0.001-10	$1.7 \times 10^{-4}$	12
Differential pulse voltammetry (Gelsolin)	0.2-40	0.05	2
Glass nanopore (Stimuli-responsive polymer)	$10^{-4}$ to 1	$10^{-4}$	This work

## References

- [1] P. Ding, X. L. Li, G. Y. Qing, T. L. Sun and X. M. Liang, *Chem. Commun.*, 2015, **51**, 16111-16114.
- [2] Y. Y. Yu, L. Zhang, C. L. Li, X. Y. Sun, D. Q. Tang and G. Y. Shi, *Angew. Chem., Int. Ed.*, 2014, **53**, 1-5.
- [3] S. S. Ding, S. M. Cao, Y. Z. Liu, Y. Lian, A. W. Zhu and G. Y. Shi, *ACS Sens.*, 2017, **2**, 394-400.
- [4] J. L. Deng, Z. H. Sheng, K. Zhou, M. X. Duan, C. Y. Yu and L. Jiang, *Bioconjugate*.

*Chem.*, 2009, **20**, 533-537.

[5] Y. Zhang, X. F. Guo, W. X. Si, L. H. Jia and X. H. Qian, *Org. Lett.*, 2008, **10**, 473-476.

[6] X. L. Xu, H. L. He and Y. D. Jin, *Anal. Chem.*, 2015, **87**, 3216-3221.

[7] R. Picou, J. Moses, A. Wellman, I. Kheterpal and S. Gilman, *Analyst*, 2010, **135**, 1631-1635.

[8] C. C. de Lassichère, T. D. Mai and M. Taverna, *J. Chromatogr. A*, 2019, **1601**, 350-356.

[9] T. Hu, C. X. Chen, G. M. Huang and X. Y. Yang, *Sens. Actuators B: Chem*, 2016, **234**, 63-69.

[10] C. Liu, D. K. Lu, X. R. You, G. Y. Shi, J. J. Deng and T. S. Zhou, *Anal. Chim. Acta.*, 2020, **1105**, 147-154.

[11] Y. Zhou, J. Liu, T. T. Zheng and Y. Tian, *Anal. Chem.*, 2020, **92**, 5910-5920.

[12] H. S. Kim, S. H. Lee and I. Choi, *Analyst*, 2019, **144**, 2820-2826.